Effects of acoustic- and optical-phonon sidebands on the fundamental optical-absorption edge in crystals and disordered semiconductors

C. H. Grein and Sajeev John
Joseph Henry Laboratories of Physics, Jadwin Hall, Princeton University, P. O. Box 708, Princeton, New Jersey 08544
(Received 1 September 1989; revised manuscript received 16 January 1990)

We present the results of a parameter-free first-principles theory for the fine structure of the Urbach optical-absorption edge in crystalline and disordered semiconductors. The dominant features are recaptured by means of a simple physical argument based on the most probable potential-well analogy. At finite temperatures, the overall linear exponential Urbach behavior of the subgap optical-absorption coefficient is a consequence of multiple LA-phonon emission and absorption sidebands that accompany the electronic transition. The fine structure of subgap absorption spectra observed in some materials is accounted for by multiple TO-, LO-, and TA-phonon absorption and emission sidebands. Good agreement is found with experimental data on crystalline silicon. The effects of nonadiabaticity in the electron-phonon interaction are calculated.

A fundamental understanding of the optical-absorption edge in crystalline and amorphous semiconductors is a long-standing problem in solid-state physics. A nearly universal feature of subgap optical absorption is Urbach's rule.[1] This empirical rule states that for photon energies $h\nu$ less than the band-gap energy, the optical-absorption coefficient takes the form

$$\alpha(\nu)\sim\exp\{[h\nu-E_G(T)]/E_0(T)\}\ , \tag{1}$$

where E_G and E_0 are temperature-dependent fitting parameters. This linear exponential behavior of the absorption coefficient may extend over ranges of photon energies up to ~ 0.5 eV corresponding to as many as five decades in α. Although this rule describes the overall features of the absorption edge, it does not account for the fine structure that is observed experimentally. We show here that both the overall features of $\alpha(\nu)$ as well as finer deviations from linearity in c-Si at finite temperatures may be quantitatively accounted for by incorporating multiple acoustic-phonon and optical-phonon sidebands.

Extensive theoretical efforts[2-18] have provided an understanding of Urbach behavior in many materials. The linear exponential behavior is due to short-range order in the static (structural or impurity) or dynamic (phonon) disorder. As was first reported by Sritrakook *et al.*,[11] an electron interacting with a static Gaussian-correlated random potential $V(x)$ with an autocorrelation function of the form $B(x)\equiv\langle V(x)(0)\rangle_{\rm ens}=V_{\rm rms}^2\exp(-x^2/L^2)$ gives rise to a linear exponential one-electron density of states (DOS) over energy ranges of experimental interest provided the correlation length L is comparable to the interatomic spacing and $V_{\rm rms}$ is of the order of 1 eV. Such an Urbach tail was not apparent in the screened Coulomb impurity model of Halperin and Lax,[2] $B(x)=V_{\rm rms}^2\exp(-|x|/L)$, for reasonable choices of L, suggesting that Urbach behavior is highly sensitive to the form of $B(x)$. Linearity in the exponential in $\alpha(\nu)$ arises from short-range order in a semiconductor that must be modeled by functions $B(x)$ of shorter range than exponential. The sensitivity of the DOS to the form and range of the autocorrelation function has been reported in Ref. 14. Because of the short time scale of optical-absorption events, lattice displacements due to thermal fluctuations (dynamic disorder) may be considered frozen in, and thus contribute to the disorder probed by the electron.

If the dipole matrix element corresponding to an electronic transition from the valence-band tail to the conduction-band tail depends only weakly on energy, then the linear exponential [$\ln\rho(E)\propto E$] behavior of the DOS will result in the optical-absorption coefficient taking form (1). The constant dipole matrix element approximation for indirect transitions is valid in many materials with large static dielectric constants,[19] including c-Si, which is the focus of this paper. In a different class of materials studied by Dow and Redfield,[4] long-range correlations do not give rise to a linear exponential DOS; however, excitonic effects lead to an electron-hole overlap matrix element that decays in a linear exponential manner, giving rise to approximate Urbach behavior in the absorption coefficient.

Recent work[17,18] has shown that the temperature dependence of the Urbach edge is accounted for by the proper consideration of longitudinal-acoustic (LA) -phonon sidebands. At finite temperatures the nonlinear electron–LA-phonon interaction gives rise to multiple phonon emission and absorption sidebands that accompany the optically induced electronic transition. The physical picture is that phonons absorbed from the heat bath are reemitted into a dynamical polaronlike potential well that localizes the electron. As we report here, the electron–longitudinal-optical (LO), –transverse-optical (TO), and –transverse-acoustic (TA) -phonon interactions also form sidebands in the absorption spectrum and are responsible for bumps in the absorption spectrum rather than the linear exponential absorption induced by LA-phonon sidebands. We believe that the derivation of the observed fine structure from a parameter-free first-principles theory, in addition to the derivation of Urbach behavior presented earlier,[17,18] provides incontrovertible evidence for the phonon-sideband model of the Urbach

edge.

In this paper we present simple formulas that go beyond previous classical potential-well results[9] and that capture the quantum-dynamical effects associated with the nonadiabatic electron-phonon interaction. These formula should be of use to experimentalists measuring subgap optical absorption since they predict the exponential part of the absorption coefficient as a function of the photon energy given a few physical parameters of the material under study. Finally, we calculate the effects of LO, TO, and TA sidebands on absorption spectra using the Feynman path-integral representation of the transition amplitude.

The exponential Urbach edge arises from three fundamental effects that provide localized electronic configurations on the time scale of an optical-absorption event. These are (i) truly static potential wells arising from impurities or structural disorder, (ii) quasistatic potential wells arising from equilibrium phonon distributions, and (iii) truly polaronic wells arising from multiple phonon absorption and emission events that are quantum-mechanically driven by the electron. The first two can be described by a most probable potential-well (MPW) method. The basis of the MPW method is the estimation of the exponential part of the band-tail density of states at a given energy by the probabiltiy of the most probable potential well that can support a bound state at this energy.[20] The approximation follows from the averaged band-tail density of states being equal to the sum over the number of potential fluctuations capable of supporting a bound state at the energy of interest times the probability of occurrence of these well. We now consider band-tail states that form as a consequence of static disorder and quasistatic wells due to equilibrium LA-phonon distributions. For various sources of disorder, the central-limit theorem implies that the probability distribution of such potential wells described by frozen-LA-phonon coordinates $q_{\mathbf{k}}$ and Fourier components of a static random potential $V(\mathbf{k})$ is given by (5.10) of Ref. 18. Following the most probable potential method discussed in Ref. 18, the lattice distortion energy is not included in order to simulate the high-temperature effects of multiple phonon absorption sidebands. Then (5.10) of Ref. 18 is an approximation to the subgap absorption coefficient for photons of energy $E+E_{\rm gap}$, where $E_{\rm gap}$ is the zero-temperature energy gap. This technique accurately accounts for the high-temperature properties of the Urbach edge, where the detailed nonadiabatic dynamics of the electron-phonon interaction are less important. However, it is not a true description of the absorption coefficient $\alpha(\nu)$, which involves a detailed enumeration of phonon-assisted electronic transitions rather than simply an effective one-electron DOS.

An approximately fit to the MPW results for a pure crystalline material ($V_{\rm rms}=0$) is obtained by considering a single oscillator mode with energy equal to the Debye energy $\hbar\omega_0\equiv\hbar u k_0$ in the most probable potential-well method. Then the Urbach slope is proportional to $E_0(T)\sim\coth(\hbar\omega_0\beta/2)$. Fitting α to the MPW results with this form of E_0 yields

$$\ln\alpha(\nu)\sim-|h\nu-E_{\rm gap}|/E_0(T)\ , \tag{2a}$$

where

$$E_0(T)\approx S_{\rm ac}\gamma^2\varepsilon_B\coth(\hbar\omega_0\beta/2)/8.4\ , \tag{2b}$$

$S_{\rm ac}\equiv E_d^2/(2Mu^2\hbar\omega_0)$, is the dimensionless electron–LA-phonon coupling constant, $\gamma\equiv\hbar\omega_0/\varepsilon_B$ is a measure of the nonadiabaticity of the electron–LA-phonon interaction, and $\varepsilon_B\equiv\hbar^2k_0^2/2m^*$.

A numerical comparison between the results of the MPW method and the results of the calculation using the Feynman path-integral representation of the transition amplitude[17,18] reveals a discrepancy that is particularly pronounced at low temperatures and weak electron–LA-phonon coupling (Fig. 1). The discrepancy is due to the MPW method not properly incorporating the nonadiabatic quantum dynamics of the electron-phonon system and the possibility of the electron driving the quantum-mechanical phonon absorption and emission processes. Over temperature and electron-phonon coupling-constant ranges of experimental interest, the MPW results are in reasonable agreement with the path-integral results in the adiabatic and small time limits,[16–18] which describes the electron localizing in static potential wells but not digging wells in the deformable lattice. We have obtained the leading-order corrections to the Urbach slope in the adiabatic and small time approximations in the limit of high temperature with no static disorder ($V_{\rm rms}=0$) and for electron–LA-phonon coupling strengths considerably below threshold for small-polaron formation ($S_{\rm ac}\gamma\approx3.5$, see Fig. 1 of Ref. 18). We find

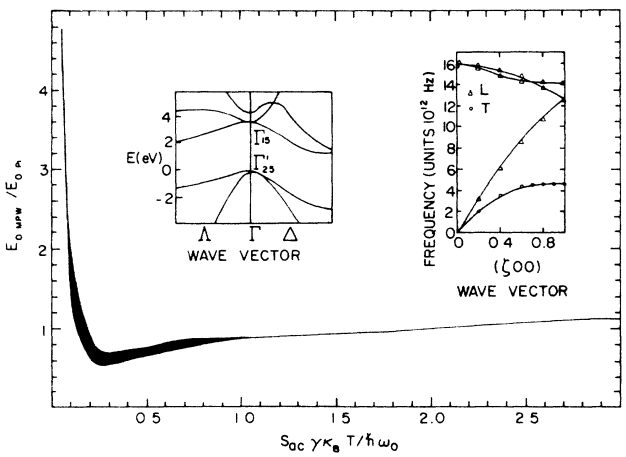

FIG. 1. The ratio of the Urbach slope E_0 calculated using most-probable potential-well (MPW) method and the general nonadiabatic path-integral (PI) method as a function of the product of the electron–LA-phonon coupling constant $S_{\rm ac}$, the nonadiabaticity parameter γ, and the temperature T. The finite width of the curve is a consequence of imperfect scaling of the ratio with respect to $S_{\rm ac}\gamma T$. The PI results are obtained with a variational trial mass. The left inset shows the electronic band structure of c-Si near the valence-band edge and the right inset shows the phonon dispersion relationships of c-Si.

$$E_0 \approx \left[S_{ac}\gamma^2 + \frac{(\hbar\omega_0\beta)^2}{S_{ac}} [0.01 - 0.06 S_{ac}\gamma + 0.08(S_{ac}\gamma)^2] \right] / (2.8\gamma\beta) \quad (3)$$

for $2\hbar\omega_0\beta \leq 1$ and $S_{ac}\gamma < 1$. The first term is obtained from the MPW method and subsequent terms are corrections from the path-integral method, clearly showing that corrections are needed to the MPW picture of the electron localizing in quasistatic potential wells arising from equilibrium phonon distributions. The correction terms were obtained by expanding the electron-phonon interaction term in power series in the small quantities $\omega_0 T_S$ and $\hbar\omega_0/\beta$, where the absorption coefficient is evaluated in the saddle-point approximation with T_S being the time at the saddle point (see Ref. 18). The dominant terms in $\omega_0 T_S$ and $\hbar\omega_0\beta$ above lowest order were retained to obtain the corrections. The lowest-order terms provide a good approximation to the MPW results. The correction terms arise from the synergetic interplay between quasistatic thermal fluctuations and polaron formation with the quasistatic fluctuations acting as nucleation centers for polaron formation.

In a material with the subgap DOS dominated by Gaussian static disorder ($V_{rms}^2 \gg S_{ac}\hbar\omega_0/2\beta$) with correlation length L comparable to the interatomic spacing, the Urbach slope may be approximated by

$$E_0 \approx \left[V_{rms}^2 + \frac{0.6 S_{ac}\hbar\omega_0}{\beta} + 0.02 S_{ac}(\hbar\omega_0)^2 - \frac{0.09 S_{ac}(\hbar\omega_0)^4}{V_{rms}^2\gamma} \right] / (14.4\epsilon_L) \quad (4a)$$

for $2\hbar\omega_0\beta \leq 1$, and

$$E_0 \approx \{ V_{rms}^2 + 0.19 S_{ac}(\hbar\omega_0)^2 [1 - 0.53(\hbar\omega_0)^2/(V_{rms}^2\gamma) + 0.23(\hbar\omega_0)^4/(V_{rms}^4\gamma^2)] \} / (14.4\epsilon_L) \quad (4b)$$

for $2\hbar\omega_0\beta \gg 1$, where $\epsilon_L \equiv \hbar^2/2m^*L^2$. In these expressions for E_0, the first two terms are due to the electron localizing in static and quasistatic thermal potential wells and the correction terms arise from the synergetic interplay between the static quasistatic fluctuations and polaron formation.

We now discuss the effects of TO-, LO-, and TA-phonon sidebands on subgap absorption spectra. Because of the inability to properly treat phonon emission and absorption process by means of the MPW method, we use the Feynman path-integral representation of the transition amplitude. In light of experimental evidence[21–24] of fine structure in the absorption of c-Si below the indirect edge, we concentrate here on c-Si, in which absorption is dominated by the valence-band tail. We consider the fine structure below the indirect edge at ~ 1.12 eV and interpret its source as being phonon sidebands forming band tails, rather than indirect optical transitions that occur for energies above the indirect edge (the case studied in Refs. 23 and 24).

The electron–LA-phonon interaction results in a shift of the valence-band edge at $\Gamma_{25'}$. In the continuum limit, the electron–LA-phonon deformation potential is given by $\Delta E_{LA} = E_d \nabla \cdot \mathbf{u}(\mathbf{r})$, where $\mathbf{u}(\mathbf{r})$ is the lattice displacement field.[25] Thus the comparatively slow (for long-wavelength phonons) spatial variation of the lattice displacement field determines the potential felt by the electron. The picture is different for optical phonons because the two sublattices vibrate against each other. The potential felt by the electron will be determined by the local relative sublattice displacement field $\mathbf{u}_{rel}(\mathbf{r})$, rather than its slow spatial modulation. Thus the long-wavelength TO- or LO-phonon deformation potential may be approximated by

$$\Delta E_{TO,LO} = |\mathbf{u}_{rel}| d_0/a \ , \quad (5a)$$

where $d_0 \sim 30$ eV (Refs. 26 and 27) for c-Si and a is the interatomic spacing. This deformation potential describes the splitting at $\Gamma_{25'}$ of the normally degenerate light- and heavy-hole bands.

The deformation-potential constant d_0 is difficult to determine experimentally; thus precise values have not been measured. One method of obtaining d_0 (Ref. 28) involves the effects of carrier concentrations on Raman frequencies. Long-wavelength optical phonons can create a dynamic redistribution of holes in the light- and heavy-hole bands. This redistribution results in a softening of the lattice and a decrease in phonon frequencies, which can be measured by Raman spectroscopy. Changing the hole concentrations by doping samples also shifts Raman frequencies. The effects of differing hole concentrations can be determined experimentally, leaving a shift of the Raman frequencies that can be related to d_0.

In terms of optical-phonon normal coordinates $\mathbf{s}_\mathbf{k}$, (5a) adds the term

$$H_{e\text{-TO,LO}} \sim \frac{d_0}{2a} \sum_{\mathbf{k}} (s_\mathbf{k} + s'_\mathbf{k} + s''_\mathbf{k}) \frac{e^{i\mathbf{k}\cdot\mathbf{r}}}{\sqrt{N}} \quad (5b)$$

to the Hamiltonian, which describes the electron–TO-phonon and -LO-phonon interactions. In (5b), the phonon normal coordinates have been written in terms of their longitudinal ($s_\mathbf{k} = \hat{\mathbf{k}} \cdot \mathbf{s}_\mathbf{k}$) and transverse ($s'_\mathbf{k}$ and $s''_\mathbf{k}$) components.

The splitting of the valence-band edge due to TA pho-

nons may be obtained through restricting a general expression linear in the strain to the symmetry of the valence-band edge.[29] The Hamiltonian takes the form

$$H_{\mathrm{TA}}=\tfrac{2}{3}D_{u'}[(J_yJ_z+J_zJ_y)\varepsilon_{yz}+\mathrm{c.p.}]\ , \tag{6}$$

where **J** is the angular momentum of the electron and

$$\varepsilon_{ij}=0.5(\partial u_i/\partial r_j+\partial u_j/\partial r_i)$$

is the strain.[30] This phenomenological expression is applicable only to the states at the top of the valence band in Si and Ge. It has been confirmed by calculations by Kleinman,[31] and describes the splitting between the heavy- and light-hole bands. For example, consider a TA phonon with wave vector in the [111] direction. Such a phonon will result in strain components $\varepsilon_{xy}=\varepsilon_{yz}=\varepsilon_{xz}=\varepsilon$ at any instant in time. Upon defining an orthogonal coordinate system with labels (1,2,3) with the quantization along the "3" direction (chosen to be the [111] direction) (6) becomes in terms of the new coordinate system

$$H_{\mathrm{TA}}=3D_{u'}\varepsilon[m_j^2-j(j+1)]=\begin{cases}-3D_{u'}\varepsilon & \text{for } m_j=\pm\frac{1}{2},\ j=\frac{3}{2}\\ 3D_{u'}\varepsilon & \text{for } m_j=\pm\frac{3}{2},\ j=\frac{3}{2}\ .\end{cases} \tag{7}$$

Thus the heavy-hole ($m_j=\pm\frac{1}{2}$) and light-hole ($m_j=\pm\frac{3}{2}$) bands split by an amount proportional to $D_{u'}$.

By averaging (6) over phonon directions in the continuum limit of the silicon lattice, and for $j=\frac{3}{2}$, the splitting may be approximated by

$$\Delta E_{\mathrm{TA}}=\frac{2D_{u'}}{3}(\varepsilon_{12}+\varepsilon_{23}+\varepsilon_{31})\ . \tag{8}$$

The lattice displacement field $\mathbf{u}(\mathbf{r})$ can be expressed in terms of its Fourier components by

$$\mathbf{u}(\mathbf{r})=\sum_{\mathbf{k}}\mathbf{q}_{\mathbf{k}}\frac{e^{i\mathbf{k}\cdot\mathbf{r}}}{\sqrt{N}}\ . \tag{9}$$

For *c*-Si, $D_{u'}\sim 2.7$ eV.[32] This deformation-potential constant can be obtained from cyclotron-resonance experiments in uniaxially strained samples. Under stress, the ligh- and heavy-hole bands split. The hole effective mass can be obtained from cyclotron resonance and can be related to the deformation potential $D_{u'}$ because the hole dispersion relationships are a function of $D_{u'}$. In terms of phonon normal coordinates, (8) adds the term

$$H_{e\text{-TA}}=\frac{iD_{u'}}{6}\sum_{\mathbf{k}}\mathbf{k}\cdot\mathbf{Q}_{\mathbf{k}}\frac{e^{i\mathbf{k}\cdot\mathbf{r}}}{\sqrt{N}}\ , \tag{10}$$

where $\mathbf{Q}_{\mathbf{k}}=(q_{\mathbf{k}2}+q_{\mathbf{k}3})\hat{1}+(q_{\mathbf{k}1}+q_{\mathbf{k}3})\hat{2}+(q_{\mathbf{k}1}+q_{\mathbf{k}2})\hat{3}$, to the Hamiltonian, which describes the electron–TA-phonon interaction. In terms of the transverse components of the TA-phonon normal coordinates ($q'_{\mathbf{k}}$ and $q''_{\mathbf{k}}$), (10) takes the form

$$H_{e\text{-TA}}=\frac{iD_{u'}}{6}\sum_{\mathbf{k}}k(q'_{\mathbf{k}}+q''_{\mathbf{k}})\frac{e^{i\mathbf{k}\cdot\mathbf{r}}}{\sqrt{N}}\ . \tag{11}$$

The deformation potentials are used to describe electron–TO-phonon, –TA-phonon, and –LA-phonon interactions and may be incorporated into the Feynman path-integral formalism discussed in Refs. 16–18. The nonlinear electron-phonon interactions will result in the formation of multiple TA- LA-, TO-, and LO-phonon absorption and emission sidebands that accompany the electronic transition. The TO- and LO-phonon sidebands are degenerate. The time contour integral that appears in this formalism must be evaluated exactly in order to properly take into account the multiple phonon emission and absorption processes. As is described in Refs. 16–18, a continuum effective-mass approximation is made for the electron and the discrete wave-vector sums appearing in (5) and (10) are replaced by integrals with soft cutoffs at the Brillouin-zone boundary. Experimentally obtained dispersion relationships are used[33] (see right inset of Fig. 1).

It is possible to obtain an analytic solution for the absorption coefficient for the case of an electron interacting only with a static Gaussian-correlated random potential and TO or LO phonons, in the infinite effective-mass (adiabatic) limit. This is a simplification of a true model for *c*-Si (equilibrium LA-phonon distributions can be modeled by a Gaussian-correlated random potential with $V_{\mathrm{rms}}^2=S_{\mathrm{ac}}k_BT\hbar\omega_0/\sqrt{2}$ and $L=\sqrt{2}\pi/k_0$, see Ref. 18); however, we present the solution here because it clearly shows how the absorption coefficient forms as a sum over sidebands, with each sideband contributing a Gaussian bump to α. The calculation is identical to the trial action method of Ref. 18, except the electron–LA-phonon deformation potential is replaced with the electron–LO-phonon or –TO-phonon deformation potential (5b) and the harmonic LA-phonon energy is replaced by

$$H_{\mathrm{op}}=M\sum_{\mathbf{k}}(|\dot{s}_{\mathbf{k}}|^2+\omega_{\mathrm{op}}^2|s_{\mathbf{k}}|^2)/2\ .$$

We consider only a single optical-phonon branch. In the infinite effective-mass approximation, one obtains

$$\alpha(\nu)=\int_{-\infty}^{\infty}e^{it(\nu-E_{\mathrm{gap}}/\hbar)}\int D\mathbf{x}(\tau)e^{iS_{\mathrm{eff}}/\hbar}\sim\int_{-\infty}^{\infty}dt\,\exp F(t)\ , \tag{12a}$$

where

$$F(t)=-\tfrac{3}{2}+it(\nu-E_{\mathrm{gap}}/\hbar-3v/2)+I_{\mathrm{int}}(t)+I_{\mathrm{dis}}(t)\ , \tag{12b}$$

$$I_{\mathrm{int}}(t)=-\frac{\pi S_{\mathrm{op}}\omega_0^3}{2k_0^3\omega_{\mathrm{op}}}\int_0^t d\Delta(t-\Delta)\int_0^{\infty}dk\,k^2\exp\left[-\frac{k^2}{k_0^2}\left[\frac{\pi}{2}+\frac{\varepsilon_B}{\hbar v}\right]\right]\{[N(\omega_{\mathrm{op}})+1]e^{-i\omega_{\mathrm{op}}\Delta}+N(\omega_{\mathrm{op}})e^{i\omega_{\mathrm{op}}\Delta}\}\ , \tag{12c}$$

and

$$I_{\rm dis}(t)=-\int_0^t d\Delta(t-\Delta)\left[\frac{V_{\rm rms}^2}{\hbar^2}\left[1+\frac{4\epsilon_L}{\hbar v}\right]^{-3/2}\right]. \tag{12d}$$

It is convenient to shift the time contour integral into the lower half complex time plane by letting $t=-iT+t'$. The absorption coefficient becomes

$$\alpha(v)\sim\omega_0\int_{-\infty}^{\infty}dt'\exp[(-T-it')A-(-T^2-2iTt'+t'^2)C+Be^{(T+it')\omega_{\rm op}}+De^{-(T+it')\omega_{\rm op}}+F]$$
$$=\sum_{m,n}e^{-[A-(n-m)\omega_{\rm op}/\omega_0]^2/4C+F}\left[\frac{\pi}{C}\right]^{1/2}\frac{B^nD^m}{n!m!}, \tag{13a}$$

where

$$A=(E_{\rm gap}-\hbar v+0.75\hbar v)/\hbar\omega_0-\frac{\pi^{3/2}S_{\rm op}(\omega_0/\omega_{\rm op})^2}{8(\pi/2+\varepsilon_B/\hbar v)^{3/2}}, \tag{13b}$$

$$B=\frac{\pi^{3/2}S_{\rm op}N(\omega_{\rm op})(\omega_0/\omega_{\rm op})^3}{8(\pi/2+\varepsilon_B/\hbar v)^{3/2}}, \tag{13c}$$

$$C=\frac{V_{\rm rms}^2}{2(\hbar\omega_0)^2(1+4\epsilon_L/\hbar v)^{3/2}}, \tag{13d}$$

$$D=\frac{\pi^{3/2}S_{\rm op}[N(\omega_{\rm op})+1](\omega_0/\omega_{\rm op})^3}{8(\pi/2+\varepsilon_B/\hbar v)^{3/2}}, \tag{13e}$$

$$F=-1.5-\frac{\pi^{3/2}S_{\rm op}[2N(\omega_{\rm op})+1](\omega_0/\omega_{\rm op})^3}{8(\pi/2+\varepsilon_B/\hbar v)^{3/2}}, \tag{13f}$$

and

$$N(\omega_{\rm op})=1/[\exp(\beta\hbar\omega_{\rm op})-1],$$

where $\omega_{\rm op}$ is the long-wavelength optical-phonon frequency, $S_{\rm op}\equiv d_0^2/2a^2M\hbar\omega_0^3$, and v is the variational frequency parameter that enters from the trial action and is chosen to maximize (13a) for each value of the photon energy $h\nu$.[18] The time contour integral appearing in the first line of (13a) can be evaluated exactly after expanding the first exponential in

$$\exp(Be^{(T+it')\omega_{\rm op}}+De^{-(T+it')\omega_{\rm op}})$$

in a power series. The result is given in the second line of (13a). With increasing photon energy, v/ω_0 increases to a value of the order of unity until the energy reaches the value at which the next lower-order phonon absorption term dominates the absorption coefficient (the kinks in the inset of Fig. 2), where it discontinuously drops to a value much less than 1 and then starts rising again. Equation (13) describes the absorption of n and the emission of m phonons, which produce bumps in the absorption spectrum (see inset of Fig. 2, where n and m are summed from 0 to 10). Terms B and D are the amplitudes for phonon absorption and emission processes, weighted by an overall factor $\exp(F)$. Term C measured the widening of the emission and absorption sideband peaks as a consequence of the electron–static-disorder interaction.

We have numerically evaluated the absorption coefficient of c-Si at 300 K taking into account electron–LA-phonon, –TA-phonon, –TO-phonon, and –LO-phonon interactions and compare this result with the experimental data of Refs. 21 and 23 in Fig. 2. We identify the bump at $\sim$1.06 eV as due to a LO- or TO-phonon absorption sideband, at energy $\hbar\omega_{\rm op}$ below the indirect edge at $\sim$1.12 eV. Reference 21 indicates that the absorption between $\sim$1.00 and 1.06 eV is enhanced by

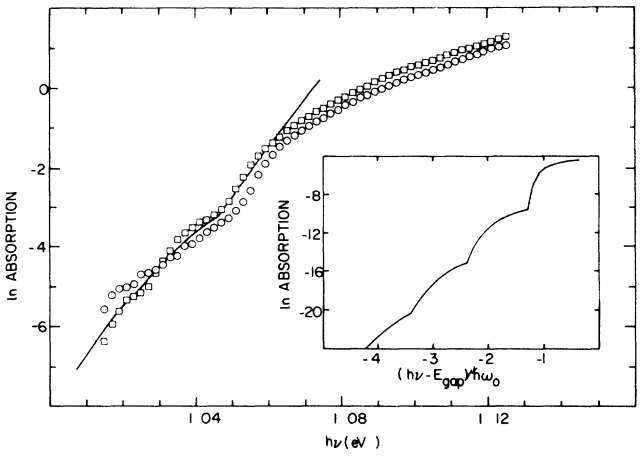

FIG. 2. Comparison of the 300-K absorption coefficient of c-Si below the indirect edge obtained from experiment [Refs. 21 (squares) and 23 (circles)] and theory (solid line). The input physical parameters are given in the text. The inset shows the absorption for an electron strongly coupled to optical phonons in the presence of static disorder, clearly displaying the optical-phonon absorption sidebands. The inset input parameters were chosen to give a clear presentation of the sidebands: The electron–TO-phonon or –LO-phonon coupling $S_{\rm op}=72$, the optical-phonon frequency scaled by the Debye frequency, $\omega_{\rm op}/\omega_0=1.23$, and the static-disorder strength $V_{\rm rms}/\epsilon_L=0.32$, where $\epsilon_L=\hbar^2/2m^*L^2$, m^* is the electron effective mass and L is the correlation length of the static disorder.

TA-phonon sidebands in addition to the optical-phonon sideband, in agreement with theory; however, the data of Ref. 23 do not display this enhancement. The theory and experiment start to diverge at higher photon energies due to the theory not incorporating indirect optical transitions above the indirect edge. Further measurements of absorption at low energies and at various temperatures would place a more stringent test on the theory.

ACKNOWLEDGMENTS

This work was supported in part by the National Science Foundation under Grant No. DMR-85-18163 at Princeton University. C. Grein acknowledges the support of the Natural Sciences and Engineering Research Council of Canada and Princeton University. We are grateful to George Cody for helpful discussions.

[1]F. Urbach, Phys. Rev. **92**, 1324 (1953); W. Martienssen, J. Phys. Chem. Solids **2**, 257 (1957).
[2]B. I. Halperin and M. Lax, Phys. Rev. **148**, 722 (1966).
[3]J. Zittartz and J. S. Langer, Phys. Rev. **148**, 741 (1966).
[4]J. D. Dow and D. Redfield, Phys. Rev. B **5**, 594 (1971).
[5]A. Sumi and Y. Toyozawa, J. Phys. Soc. Jpn. **31**, 342 (1971).
[6]T. Skettrup, Phys. Rev. B **18**, 2622 (1978).
[7]M. Schreiber and Y, Toyozawa, J. Phys. Soc. Jpn. **51**, 1544 (1982).
[8]J. L. Cardy, J. Phys. C **11**, L321 (1978).
[9]S. John, C. Soukoulis, M. H. Cohen, and E. N. Economou, Phys. Rev. Lett. **57**, 1777 (1986).
[10]V. Sa-yakanit, Phys. Rev. B **19**, 2266 (1979).
[11]W. Sritrakool, V. Sa-yakanit, and H. R. Glyde, Phys. Rev. B **33**, 1199 (1986).
[12]C. T. Chan, S. G. Louie, and J. C. Phillips, Phys. Rev. B **35**, 2744 (1987).
[13]S. John, Phys. Rev. B **35**, 9291 (1987).
[14]S. John, M. Y. Chou, M. H. Cohen, and C. M. Soukoulis, Phys. Rev. B **37**, 6963 (1988).
[15]S. John and M. H. Cohen, Phys. Rev. B **34**, 2428 (1986).
[16]C. H. Grein and S. John, Phys. Rev. B **35**, 7457 (1987).
[17]C. H. Grein and S. John, Solid State Commun. **70**, 87 (1989).
[18]C. H. Grein and S. John, Phys. Rev. B **39**, 1140 (1989).
[19]J. Ingers, K. Maschke, and S. Proennecke, Phys. Rev. B **37**, 6105 (1988).
[20]S. John and M. J. Stephen, J. Phys. C **17**, L559 (1984).
[21]G. Cody and B. Brooks (private communication).
[22]A. Frova, P. Handler, F. A. Germano, and D. E. Aspens, Phys. Rev. **145**, 575 (1966).
[23]G. G. MacFarlane, T. P. McLean, J. E. Quarringron, and V. Roberts, Phys. Rev. **111**, 1245 (1958).
[24]F. A. Johnson, Proc. Phys. Soc. London **73**, 265 (1959).
[25]S. John and M. H. Cohen, Phys. Rev. B **34**, 2428 (1986).
[26]W. Pötz and P. Vogl, Phys. Rev. B **24**, 2025 (1981).
[27]A. Blacha, H. Presting, and M. Cardona, Phys. Status Solidi B **126**, 11 (1984).
[28]F. Cereira and M. Cardona, Phys. Rev. B **5**, 1140 (1971).
[29]W. H. Kleiner and L. M. Roth, Phys. Rev. Lett. **2**, 334 (1959).
[30]J. C. Hensel and G. Feher, Phys. Rev. **129**, 1041 (1963).
[31]L. Kleinman, Phys. Rev. **128**, 2614 (1962).
[32]I. Goroff and L. Kleinman, Phys. Rev. **132**, 1080 (1963).
[33]*Inelastic Scattering of Neutrons in Solids and Liquids* (IAEA, Vienna, 1963), Vol. II.